Thermoelectric signature of Majorana zero modes in a T-typed double-quantum-dot structure

Cong Wang(王聪) and Xiao-Qi Wang(王晓琦)†

Basic Department, Yingkou Institute of Technology, Yingkou 115014, *China*

(Received 17 February 2022; revised manuscript received 10 September 2022; accepted manuscript online 19 September 2022)

The thermoelectric effect of the system is theoretically investigated, by coupling Majorana zero mode to the T-typed double-quantum-dot-structure in different ways. It is found that when a single Majorana zero mode is coupled to one of the quantum dots (QDs), the thermoelectric efficiency is suppressed due to the leakage of Majorana zero modes into the QDs. When the Majorana zero mode is coupled to QD2, the suppression of the thermoelectric efficiency is more serious than that of QD1. Furthermore, when two Majorana zero modes are introduced simultaneously, suppression of the thermoelectric effect still takes place. We believe that such results can be candidates for the detection of Majorana bound states and help us understand the role of Majorana zero mode in thermoelectricity.

Keywords: Majorana bound state, thermoelectricity, quantum dots, figure of merit

PACS: 73.21.–b, 74.45.+c, 74.55.+v, 72.10.Bg **DOI:** 10.1088/1674-1056/ac92d3

1. Introduction

Recently, interest in thermoelectric phenomena in quantum dot systems has rapidly increased since strong violation of the Wiedemann–Franz law and small phonon contribution to thermal conductance, which leads to significant improvement of the thermoelectric effect.[1,2] More recently, some research groups have focused on the thermoelectric effect in multi-QD systems.[3–8] This is because the more diverse pathways and interference effects provided by the multi-QD structure greatly affect the thermoelectric properties. For example, in the T-typed double QD system, the thermopower exhibits maxima for temperatures corresponding to the second stage of screening.[9] In the nonlinear regime of transport, nontrivial zeros and negative differential conductances will take place for parallel-coupled double QD due to the applied thermal gradient.[7] For triple QD structure, the Dicke effect is dominant, and the thermoelectric efficiency is strongly affected by the Dicke effect which can be controlled by the level shift, interdot tunneling coupling, and Coulomb interaction.[5] And finally, when additional magnetic fields are present in the QD system, we have to consider the influence of spin polarization on the thermoelectric effect, i.e., spin thermoelectric effects, which have been investigated in detail by some research groups.[10–12]

Nowadays, both the theoretical and experimental aspects of the Majorana bound state (MBS) at the end of the topological superconductor have attracted considerable interest in the field of condensed matter physics,[13–19] because of the important applied value of its zero modes, i.e., the fault-tolerant quantum computation with qubits.[13–15] As a result, how to detect the Majorana zero mode (MZM) is very important. According to the relevant reports, various candidates for detecting MZM have been designed. For instance, zero-bias charge conductance peak is a marked feature of MZM, which is a simple but effective method for detections of MZM, i.e., when a lead couples to an isolated Majorana island, the Majorana fermions induce resonant Andreev reflections will be happened, which leads to a robust quantized zero-bias differential conductance of $2e^2/h$.[20] The fractional Josephson effect in topological superconductors (TSs) is also a shred of strong evidence for the existence of MZM.[21] Besides, due to the controllability of QDs, it is also a feasible scheme to detect Majorana by using QDs.[22] Recently, a feasible empirical protocol for detecting MZM utilizing the time-resolved Andreev tunneling spectroscopy has also been proposed.[23]

It is the development of the MBS and the thermoelectric effect in their respective fields that has led to the widespread interest in MBS-driven thermoelectric effect. First, In one single-QD structure coupled to two TSs nanowires system, a notable thermoelectric effect takes place when two MZMs are introduced simultaneously.[24] Next, van Dalum *et al.* found that in a non-Fermi liquid and Majorana central charge, fractionalized Majorana character of the critical point can be unambiguously detected from the heat conductance.[25] The other group discussed nonequilibrium thermoelectric quantum noise. It has been observed that at finite frequency ω MZMs induce a perfect universal symmetry between photon emission and absorption spectra and produce universal thermoelectric resonances in their frequency dependence in contrast to non-Majorana quantum noise which is either asymmetric or nonuniversal.[26]

†Corresponding author. E-mail: yklgwxq@163.com

© 2023 Chinese Physical Society and IOP Publishing Ltd

The previous reports have shown that the MBS-driven thermoelectric effect is indeed important and deserves further investigation. Following this line of thought, in the present work we consider the structure of two topological superconductors coupled to a T-typed double QD and study the thermoelectric properties therein. As a typical case, we are mainly interested in the case of Majorana zero mode. After calculations, we find that the thermoelectric efficiency is severely suppressed if a single MZM is coupled to one of the two QDs. The thermoelectric efficiency is more severely suppressed in the case of coupling to QD2 than that in the case of coupling to QD1. We believe that such results can be candidates for the detection of MBSs and help us understand the role of MZM in thermoelectricity.

2. Model

The T-typed double QD thermoelectric structure that we considered is illustrated in Fig. 1. Two topological superconductors hosting MBSs at its ends are coupled to the QD2 and the QD1, respectively.

The considered system of Fig. 1 can be described by the following Hamiltonian:

$$\mathcal{H} = H_\alpha + H_{\rm M} + H_{\rm D} + H_{\rm T}, \tag{1}$$

the first term describes the left and the right normal metallic lead

$$H_\alpha = \sum_{\alpha={\rm L,R}} \sum_{k\sigma} \varepsilon_{\alpha k} c^\dagger_{\alpha k\sigma} c_{\alpha k\sigma}, \tag{2}$$

where $c^\dagger_{\alpha k\sigma}$ ($c_{\alpha k\sigma}$) is an operator to create (annihilate) an electron with spin σ, momentum k and energy $\varepsilon_{\alpha k}$ of the continuous state $|\alpha k\sigma\rangle$ in the normal metallic lead-α.

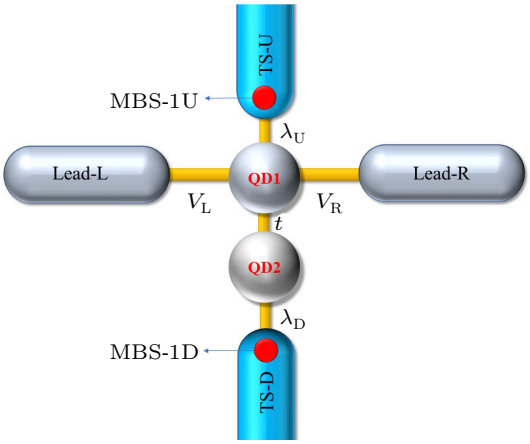


Fig. 1. Sketch of the thermoelectric system induced by the MZM.

The second term of H represents the Hamiltonian for the MBS. In this work, we would like to present its low-energy effective form, which can be written as

$$H_{\rm M} = {\rm i} \sum_{n={\rm U,D}} \varepsilon_{mn} \eta_{1n} \eta_{2n}, \tag{3}$$

here, η_{1n} (η_{2n}) is the self-Hermitian operator for the 1st (2nd) MBS in the nth ($n = {\rm U,D}$) topological superconductor nanowire with $\eta_{1n} = \eta^\dagger_{1n}$ ($\eta_{2n} = \eta^\dagger_{2n}$). ε_{mn} describes degree of the overlap between the wave functions of two Majorana quasiparticles in nth TS. Once the length of the Majorana wire is much larger than the superconducting coherence length, there is no overlap between the two Majorana quasiparticles ($\varepsilon_{mn} = 0$). On the contrary, ε_{mn} is finite, which results in a splitting of the energies of the Majorana quasiparticles.[27]

The QD's Hamiltonian with their couplings $H_{\rm D}$ reads

$$H_{\rm D} = \sum_{i=1,2} \sum_\sigma \varepsilon_{i\sigma} d_{i\sigma} d^\dagger_{i\sigma} + \sum_\sigma t (d^\dagger_{1\sigma} d_{2\sigma} + d^\dagger_{2\sigma} d_{1\sigma}), \tag{4}$$

where $d_{i\sigma}$ ($d^\dagger_{i\sigma}$) is creation (annihilation) operator in the ith QDs. $\varepsilon_{i\sigma}$ models ith QD's level with spin index σ ($\sigma = \pm$ or $\uparrow\downarrow$). t is the hopping matrix element between two QDs.

Finaly, the last term of H models couplings between QD and MBS, and electron transition between QD and normal metallic leads. It takes the form

$$\begin{aligned} H_{\rm T} = {} & (\lambda_{\rm U} d^\dagger_{1\uparrow} - \lambda_{\rm U} d_{1\uparrow}) \eta_{1{\rm U}} + (\lambda_{\rm D} d^\dagger_{2\uparrow} - \lambda_{\rm D} d_{2\uparrow}) \eta_{1{\rm D}} \\ & + \sum_{\alpha k} V_\alpha c^\dagger_{\alpha k\sigma} d_{1\sigma} + {\rm h.c.}, \end{aligned} \tag{5}$$

where $\lambda_{\rm U}$ ($\lambda_{\rm D}$) is coupling coefficient between TS-U (TS-D) and the QD1 (QD2). V_α represents coupling between QD1 and lead-α.

With respect to such a structure, we would like to present a comprehensive analysis on its thermoelectric properties in the linear-response regime. For this purpose, we introduce temperature gradient δT to apply symmetrically between lead-L and lead-R, i.e., $T_{\rm L} = T - \delta T/2$ and $T_{\rm R} = T + \delta T/2$, while the TSs are kept at temperature T. According to thermoelectric theory, the electric and hot current in the linear response regime can be deducted in terms of the temperature gradient δT and a voltage δV,

$$I_e = L_{11}\delta V + L_{12}\delta T, \quad I_Q = L_{21}\delta V + L_{22}\delta T. \tag{6}$$

The transport coefficients L_{ij} can be expressed in terms of the transport integral

$$J_n = \frac{1}{h} \int \left(-\frac{\partial f}{\partial \omega} \right) (\omega - \mu)^n \mathcal{T}(\omega) {\rm d}\omega \tag{7}$$

as $L_{11} = e^2 J_0$, $L_{21} = -eJ_1$, $L_{12} = -eJ_1/T$, and $L_{22} = J_2/T$. μ is the system's chemical potential at equilibrium. For the symmetric QD–lead coupling, the the voltage will distribute symmetrically with $\mu_{\rm L(R)} = \pm e(\delta V/2)$ ($\delta V = V_{\rm L} - V_{\rm R}$). $\mathcal{T}(\omega)$ is the transmission function. According to the quantum transport

theory, the transmission spectra $\mathcal{T}(\omega)$ obeys the following expression:

$$\mathcal{T}(\omega) = -\Gamma \mathrm{Im} G^{\mathrm{R}}_{11}, \tag{8}$$

where $\Gamma_\alpha = 2\pi |V_\alpha|^2 \rho(\omega)$ describes the coupling between the QD and lead-α. In this work we only take our interest in the case of symmetric QD–lead coupling, so there will be $\Gamma_{\mathrm{L}} = \Gamma_{\mathrm{R}} = \Gamma$. By a straightforward derivation, we can obtain the matrix form of the retarded Green function in our considered structure with two topological superconductors

$$G^{\mathrm{R}}(\omega) = \begin{pmatrix} \omega-\varepsilon_1+\mathrm{i}\Gamma & 0 & -t & 0 & -\lambda_{\mathrm{U}} & 0 & 0 & 0 \\ 0 & \omega+\varepsilon_1+\mathrm{i}\Gamma & 0 & t & \lambda_{\mathrm{U}} & 0 & 0 & 0 \\ -t & 0 & \omega-\varepsilon_2 & 0 & 0 & 0 & -\lambda_{\mathrm{D}} & 0 \\ 0 & t & 0 & \omega+\varepsilon_2 & 0 & 0 & \lambda_{\mathrm{D}} & 0 \\ -\lambda_{\mathrm{U}} & \lambda_{\mathrm{U}} & 0 & 0 & 0 & -\mathrm{i}\varepsilon_{m1} & 0 & 0 \\ 0 & 0 & 0 & 0 & \mathrm{i}\varepsilon_{m1} & 0 & 0 & 0 \\ 0 & 0 & -\lambda_{\mathrm{D}} & \lambda_{\mathrm{D}} & 0 & 0 & 0 & -\mathrm{i}\varepsilon_{m2} \\ 0 & 0 & 0 & 0 & 0 & 0 & \mathrm{i}\varepsilon_{m2} & 0 \end{pmatrix}^{-1}. \tag{9}$$

Then liner conductance $\mathcal{G} = \lim_{V\to 0} \mathrm{d}I_e/\mathrm{d}V = L_{11}$ is given by equation

$$\mathcal{G} = e^2 J_0. \tag{10}$$

The thermopower of a QD system in a configuration with two normal leads can be found in an open circuit by measuring the induced voltage drop across a QD when the temperature difference is applied between the two leads. The thermopower is defined by the relation

$$S = -\frac{\delta V}{\delta T}|_{I=0}, \tag{11}$$

and can be expressed as

$$S = -\frac{1}{eT}\frac{J_1}{J_0}. \tag{12}$$

The electronic contribution to the thermal conductance defined by $\kappa_e = \delta I_{\mathrm{Q}}/\delta T$ can be given by

$$\kappa_e = J_1 e S + \frac{J_2}{T}. \tag{13}$$

Based on these formulas, the thermoelectric efficiency in such a structure can be evaluated, since its corresponding figure of merit is defined as

$$ZT = \frac{S^2 \mathcal{G} T}{\kappa_e + \kappa_{\mathrm{p}}}, \tag{14}$$

in which the phonon-contributed thermal conductance has been ignored, i.e., $\kappa_{\mathrm{p}} = 0$. Such an approximation is reasonable since the phonon transport can be seriously suppressed due to the strong interface scattering in the QD structures.[28,29]

3. Numerical results and discussion

With the theory in the above section, we begin to perform the numerical calculation to investigate the thermoelectric properties driven by the MBSs in T-typed double QD structure with two TSs. In this paper, we keep the energy levels of the two QDs consistent, i.e., $\varepsilon_1 = \varepsilon_2 = \varepsilon_0$. In addition, we take the coupling coefficient Γ between QD2 and leads as the unit. Γ can be regarded as 0.1 meV according to the relevant experiments.[30,31]

First of all, we ignore the QD-MZM coupling to present the thermoelectric properties of the T-typed double QDs system. In this situation, the relevant numerical results are shown in Fig. 2. For comparison, the temperature is set to 0.04 and 0.1. As for coupling between QDs, we take it to be 0.5, 1.0, and 2.0, respectively. In Fig. 2(a), one can find that the maximum of electronic conductance appears at the position of $\varepsilon_0 = \pm t$, and that the conductance spectrum is an even function symmetric about $\varepsilon_0 = 0$. As t increases, an obvious anti-resonance point appears at the vicinity of $\varepsilon_0 = 0$, and the width of the anti-resonance region gradually increases, which is attributed to quantum destructive interference effects between the two QDs. Nevertheless, compared to the case with $k_{\mathrm{B}}T = 0.1$, the anti-resonance phenomenon appears earlier at $k_{\mathrm{B}}T = 0.04$. At low temperature, the thermal conductance is mainly dominated by the contribution of electron and thus depends on the transmission function. As a result, the thermal conductance in Fig. 2(b) exhibits a similar phenomenon except that when the interdot coupling is weak (but nonzero), the thermal conductance has a peak at $\varepsilon_0 = 0$. In Fig. 2(c), it can be clearly seen that the thermopower changes from negative to positive as the energy level of the QDs increases, due to the change in carriers from electrons to holes. In addition, the magnitude of the Seebeck coefficient increases following the increment of interdot coupling. The maximum Seebeck coefficient occurs near the anti-resonance point and its position is related to temperature. The extremum of ZT (figure of merit)

reflects the thermoelectric efficiency, and its result is shown in Fig. 2(d). It can be seen that, analogous to the thermopower, the value of ZT gradually increases with the enhancement of the coupling between the two QDs, reaching a maximum value of ZT when $t = 1.0$ and $k_BT = 0.1$, and the maximum value exceeds 1.2.

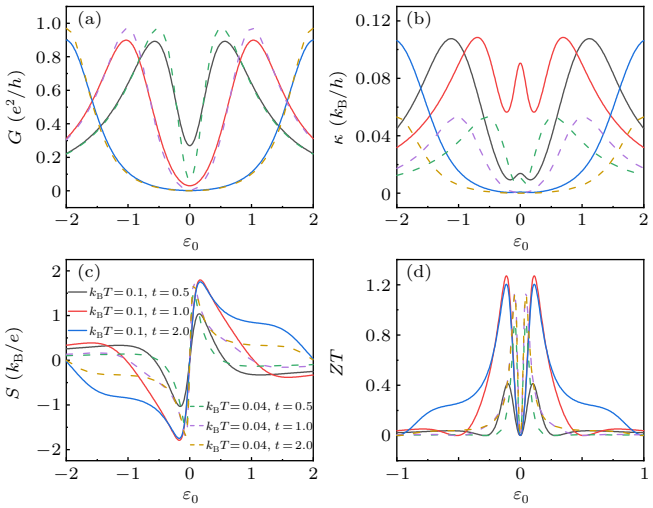


Fig. 2. Thermoelectric quantities of T-typed double QD structure as functions of the QD level ε_0, in the absence of QD-MZM couplings. (a)–(d) The numerical results of the electronic conductance, thermal conductance, thermopower, and figure of merit. Coupling coefficient between two QDs $t = 0.5$, 1.0, 2.0. The other relevant parameters are taken to be $k_BT = 0.04$ and $k_BT = 0.1$, respectively.

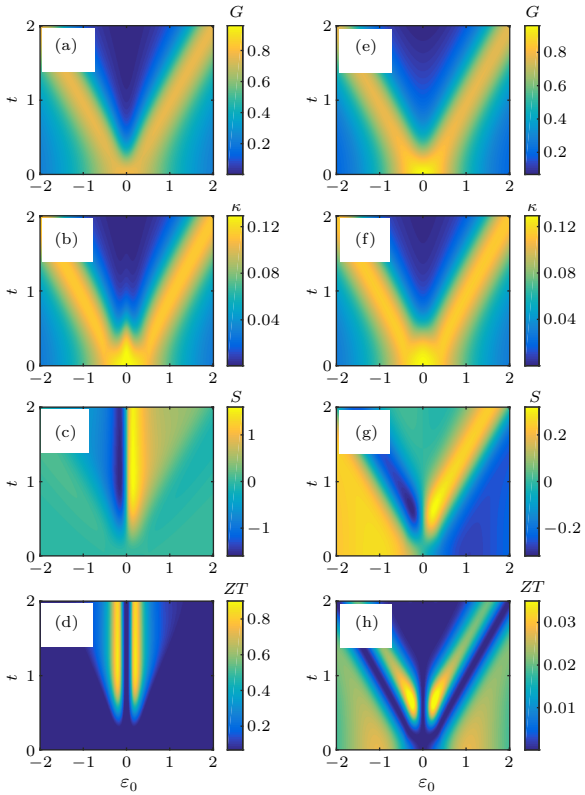


Fig. 3. Spectra of thermoelectric quantities of the T-typed double-quantum-dot structure, when one MBS is coupled to QD. The temperature are taken to be $k_BT = 0.1$. QD-MBS coupling is assumed to be $\lambda = 0.2$. The left column describes situation which one MBS is coupled to QD1, the right column corresponds to QD2.

Next, we couple a single MZM to T-typed double QD structure and investigate the influence of the MZM on the thermoelectric effect. In this part, we take $k_BT = 0.1$. The left column in Fig. 3 shows the effect of interdot coupling on the thermoelectric properties when TS-U is coupled to QD1, taking $\lambda_U = 0.2$. From Figs. 3(a)–3(d), we can observe that for $t = 0$, a peak at $\varepsilon_0 = 0$ appears in electronic conductance and thermal conductance spectra, and the anti-resonance phenomenon is shown in the electronic conductance and thermal conductance spectra with increasing interdot coupling strength, due to the existence of the quantum interference effects.[32] Meanwhile, the Seebeck coefficient and figure of merit are increased to about 1.5 and 1, respectively. When the MZM is coupled to QD2 ($\lambda_D = 0.2$), the electronic conductance and thermal conductance also exhibit anti-resonance phenomena. However, the numerical results for the thermopower and ZT are completely different from those for the TS-U coupling to QD1. Regardless of the interdot coupling variations, λ_D severely suppresses the values of ZT and Seebeck coefficients.

To further clarify the difference between the above two situations in the T-typed double QD structure, we fixed the interdot coupling at 0.6 to research the effect of the MZM-QD coupling strength on the thermoelectric effect. Comparing Figs. 4(a) and 4(e), we can find that when MBS-1U is coupled to the QD1, the increase of MZM-QD coupling does not modify the anti-resonance near $\varepsilon_0 = 0$ in Fig. 4(a). However, the results in Fig. 4(e) are completely different. That is, when λ_D increases to about 0.5, the anti-resonance phenomenon disappears completely, and then the conductance value tends to $1/2$. The same phenomenon also occurs in the thermal conductance results of Figs. 4(b) and 4(f). The reason for the above results is that although MBS-1U leak into the QDs, it does not destroy the quantum interference effect in the structure, while the MBS-1D not only leak into the system but also completely suppressed the quantum interference effect, leading to the disappearance of anti-resonance. To confirm the above idea, we try to give the analytical solution of the system. We do not consider the coupling between MBSs, i.e. $\varepsilon_{m1} = 0$, $\varepsilon_{m2} = 0$. Furthermore, we only focus on the anti-resonance point ($\varepsilon_0 = 0$), then Eq. (9) can be simplified to

$$G^{\mathrm{R}}(\omega) = \begin{pmatrix} g & 0 & -t & 0 & -\lambda_U & 0 \\ 0 & g & 0 & t & \lambda_U & 0 \\ -t & 0 & \omega & 0 & 0 & -\lambda_D \\ 0 & t & 0 & \omega & 0 & \lambda_D \\ -\lambda_U & \lambda_U & 0 & 0 & 0 & 0 \\ 0 & 0 & -\lambda_D & \lambda_D & 0 & 0 \end{pmatrix}^{-1}, \quad (15)$$

in which $g = \omega + \mathrm{i}\Gamma$. When TS-U (TS-D) is involved in the

structure, transmission function can be written as

$$\mathcal{T}_{\rm U}(\omega)=\frac{\omega^2\Gamma^2(2\lambda_{\rm U}^4+2\lambda_{\rm U}^2A+A^2+\omega^2\Gamma^2)}{(A^2+\omega^2\Gamma^2)((2\lambda_{\rm U}^2+A)^2+\omega^2\Gamma^2)}, \tag{16}$$

$$\mathcal{T}_{\rm D}(\omega)=\frac{\Gamma^2(\omega^4A^2+\omega^6\Gamma^2-2\lambda_{\rm D}^2\omega^2(B-t^2\omega^2)+2\lambda_{\rm D}^4B)}{(A^2+\omega^2\Gamma^2)(\omega^2(2\lambda_{\rm D}^2+A)^2+\Gamma^2(\omega^2-2\lambda_{\rm D}^2)^2)}, \tag{17}$$

respectively, in which $A=t^2-\omega^2$ and $B=t^4-2t^2\omega^2+2\omega^2(\omega^2+\Gamma^2)$. we find that when $\omega=0$, $\mathcal{T}_{\rm U}=0$, and $\mathcal{T}_{\rm D}=1/2$. The above theoretical analysis is in good agreement with the results of Figs. 4(a) and 4(e). In general, the magnitude of the thermopower and ZT depend on the sharp change in transmission function.[5] On the one hand, we can observe that the thermopower and ZT are suppressed when TS-U is coupled to QD1. This is because MZM leakage into the quantum dots suppresses the change in the transmission spectrum. On the other hand, when TS-D is coupled to QD2, the thermopower and ZT are severely suppressed due to the disruption of the quantum interference effect. And the relevant results are shown in Figs. 4(c)–4(d) and 4(g)–4(h). Next, we investigate the effect of conventional superconductors on the thermoelectric effect using s-wave superconductors instead of TS-U. In this case, the QD Hamiltonian can be written as $H_{\rm D}=\sum_{i=1,2}\sum_\sigma\varepsilon_{i\sigma}d_{i\sigma}d_{i\sigma}^\dagger+\sum_\sigma t(d_{1\sigma}^\dagger d_{2\sigma}+d_{2\sigma}^\dagger d_{1\sigma})-\Delta_d d_{1\uparrow}^\dagger d_{1\downarrow}^\dagger+{\rm h.c.}$ Here the superconducting-pairing potentials in the superconductors have been supposed to be infinity, and $\Delta_d=\pi\sum_k|V_k|^2\rho_{\rm s}$ in which $\rho_{\rm s}$ is the density of state in the superconductors and V_k is the superconductor–QD coupling coefficient. The numerical results are shown in Fig. 5. It can be noticed that the figure of merit and thermopwer can be only suppressed slightly by the increase of superconductor–QD coupling compared to the case of topological superconductor. Up to now, it is not difficult for us to understand the role of MZM in T-typed-double-QD structure and we belive T-typed-double-QD structure with TS-U can be a feasible alternative for the detection of Majorana bound states.

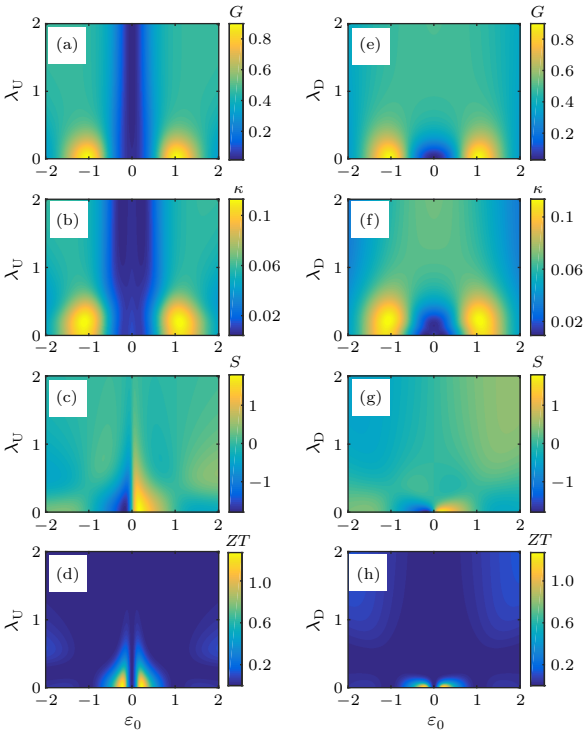


Fig. 4. Thermoelectric quantities of T-typed double-quantum-dot structure, as functions of the QD level ε_0. when one MBS is coupled to QD. The interdot coupling is taken to be $t=0.6$. The left column describes situation which one MBS is coupled to QD1, the right column corresponds to QD2. The other relevant parameters are the same as Fig. 3.

Finally, in Fig. 6 we consider the case that TS-U and TS-D are coupled to the system at the same time. The first observation is that with the increase of QD-MZM coupling strength, the antiresonance peak in the conductance spectrum is suppressed, which further shows that the TS-D is the reason for affecting the quantum interference effect. However, it is worth mentioning that the thermopower and ZT have not been greatly enhanced as in Ref. [24]. The relevant results are shown in Figs. 6(c) and 6(d).

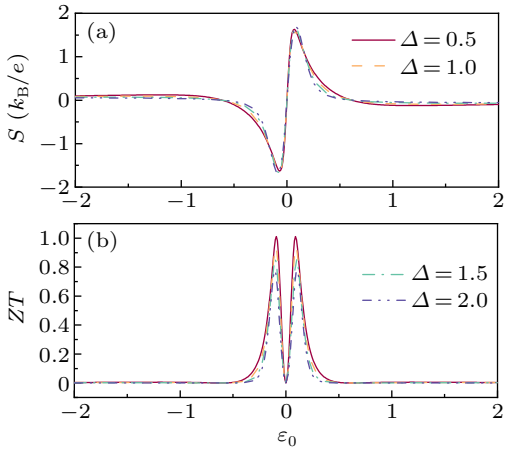


Fig. 5. Thermoelectric quantities of T-typed double-quantum-dot structure when the TS-U are chosen to be s-wave superconductor. The interdot coupling is taken to be $t=0.6$.

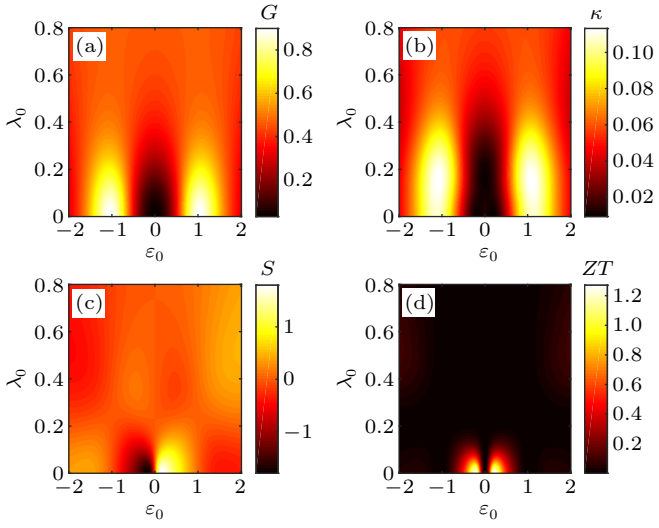


Fig. 6. Spectra of thermoelectric quantities of the T-typed double-quantum-dot structure, when two MBSs are coupled to QD at the same time. The temperature are taken to be $k_{\rm B}T=0.1$. The interdot coupling is assumed to be $t=0.6$.

4. Summary

In summary, we have calculated the influence of MZMs on thermoelectric quantities, by considering them to couple to QD1 and the QD2. As a result, it has been found that the Majorana zero modes take effect to modify thermoelectric quantities. On the one hand, compared to the case of a normal superconductor, the thermopower and ZT are suppressed more severely with increasing QD-MZM coupling when TS-U is coupled to the system. On the other hand, when TS-D is introduced, the suppression of thermoelectric efficiency is more pronounced due to the destruction of quantum interference effects. We believe that all these findings provide new information for understanding the MZM-induced thermoelectric effect in the experiment and provide a thermoelectric candidate for the detection of Majorana bound states.

Acknowledgments

Project supported by High-level talents research project of Yingkou Institute of Technology (Grant No. YJRC202027) and the Natural Science Foundation of Liaoning Province of China (Grant No. 2020-BS-287).

References

[1] Harmanp T C, Taylorm J, Walshand P and Laforge B E 2002 *Science* **297** 2229
[2] Zhang Y, Lin G and Chen J 2015 *Phys. Rev. E* **91** 052118
[3] Thierschmann H, Sánchez R, Sothmann B, Arnold F, Heyn C, Hansen W, Buhmann H and Molenkamp L W 2015 *Nat. Nanotech.* **10** 854
[4] Zhang Y, Zhang X, Ye Z, Lin G and Chen J 2017 *Appl. Phys. Lett.* **110** 153501
[5] Wang Q, Xie H, Nie Y and Ren W 2013 *Phys. Rev. B* **87** 075102
[6] Juergens S, Haupt F, Moskalets M and Splettstoesser J 2013 *Phys. Rev. B* **87** 245423
[7] Sierra M A, Saiz-Bretín M, Domínguez-Adame F and Sánchez D 2016 *Phys. Rev. B* **93** 235452
[8] Wierzbicki M and Swirkowicz R 2011 *Phys. Rev. B* **84** 075410
[9] Wójcik K P and Weymann I 2016 *Phys. Rev. B* **93** 085428
[10] Tang G, Thingna J and Wang J 2018 *Phys. Rev. B* **97** 155430
[11] Weymann I and Barnaś J 2013 *Phys. Rev. B* **88** 085313
[12] Karwacki Ł and Trocha P 2016 *Phys. Rev. B* **94** 085418
[13] Nayak C, Simon S H, Stern A, Freedman M and Das Sarma S 2008 *Rev. Mod. Phys.* **80** 1083
[14] Wilczek F 2009 *Nat. Phys.* **5** 614
[15] Stern A 2010 *Nature* **464** 187
[16] Ramos-Andrade J P, Orellana P A and Vernek E 2020 *Phys. Rev. B* **101** 115403
[17] Legg H F, Loss D and Klinovaja J 2021 *Phys. Rev. B* **104** 165405
[18] Manousakis J, Wille C, Altland A, Egger R, Flensberg K and Hassler F 2020 *Phys. Rev. Lett.* **124** 096801
[19] Mao Y and Sun Q 2021 *Phys. Rev. B* **103** 115411
[20] Nichele F, Drachmann A C C, Whiticar A M, *et al*. 2017 *Phys. Rev. Lett.* **119** 136803
[21] Chiu C and Das Sarma S 2019 *Phys. Rev. B* **99** 035312
[22] Cifuentes J D and Dias da Silva L G G V 2019 *Phys. Rev. B* **100** 085429
[23] Barański J, Barańska M, Zienkiewicz T, Taranko R and Domański T 2021 *Phys. Rev. B* **103** 235416
[24] Wang X Q, Zhang S F, Han Y, Yi G Y and Gong W J 2019 *Phys. Rev. B* **99** 195424
[25] van Dalum G A R, Mitchell A K and Fritz L 2020 *Phys. Rev. B* **102** 041111
[26] Smirnov S 2019 *Phys. Rev. B* **100** 245410
[27] Cronenwett S M, Oosterkamp T H and Kouwenhoven L P 1998 *Science* **281** 540
[28] Harman T C, Taylor P J, Walsh M P and LaForge B E 2002 *Science* **297** 2229
[29] Reddy P, Jang S Y, Segalman R A and Majumdar A 2007 *Science* **315** 1568
[30] Vernek E, Penteado P H, Seridonio A C and Egues J C 2014 *Phys. Rev. B* **89** 165314
[31] Mourik V, Zuo K, Frolov S M, Plissard S R, Bakkers E P A M and Kouwenhoven L P 2012 *Science* **336** 1003
[32] Xu T T, Gong T, Zhang L L and Gong W J 2022 *Physica E* **143** 115397